RESEARCH ARTICLE

CrossMark

Air pollution control and flue gas desulfurization residues from Polish copper smelting facility as adsorbents of Pb(II) and Cu(II) from aqueous solutions

Bartosz Mikoda[1] (iD) · Agnieszka Gruszecka-Kosowska[1] · Agnieszka Klimek[1] · Anna Tomczyk[1]

Abstract

This study aimed at evaluation of air pollution control residues (APCR) and flue gas desulfurization residues (FGDR) from copper foundry in Southwestern Poland as adsorbents of Cu(II) and Pb(II) from simulated wastewater. Studies of the impact of pH and adsorbent dose, as well as sorption isotherms, and kinetic and thermodynamic studies were conducted in a series of batch experiments. The maximum adsorption capacities were equal to 42.9 mg g^{-1} Cu(II) and 124.4 mg g^{-1} Pb(II) for APCR and 98.8 mg g^{-1} Cu(II) and 124.7 mg g^{-1} Pb(II) for FGDR, which was comparable to mineral adsorbents examined in other studies. Adsorption isotherms followed the Langmuir model, except for Pb(II) for FGDR, which followed Freundlich model. Sorption kinetics for both materials was properly expressed by pseudo-second-order equation. Mean adsorption energy parameter suggested that the adsorption might have occurred via physical bonding. Thermodynamic study revealed that adsorption was spontaneous and endothermic for Cu(II) and not spontaneous and exothermic for Pb(II), with lower temperature favoring the process. The results suggested that both materials had high affinity towards Cu(II) and Pb(II) ions and could be conducted industrial scale research for consideration as potential adsorbents from aqueous solutions.

Keywords Heavy metals · Copper waste · Low-cost adsorbents · Wastewaters · Adsorption isotherms · Sorption experiments

Introduction

The increasing human activity and technology development are beneficial for mankind; the environmental conditions, however, suffer from it more and more visibly. The pollutants resulting from industrial processes pose threat to biota and non-living part of ecosystems (water, soil, etc.). Heavy metals and metalloids are one of the representative groups of pollutants with scientifically evidenced impact on the global and local scales. One of the most abundant metals in industrial run-offs is copper and lead. The main sources of Cu and Pb from industrial activity are mining, power engineering, metal smelting, radiator manufacturing, and alloy industries (Adriano, 2001; Kadirvelu et al. 2001; Hua et al. 2012). Risk for humans is associated with ability of these metals to disperse in water systems and migrate within them, which is one of the most important paths of exposure since metals accumulate easily in living tissues (Liu et al. 2010; Tchounwou et al. 2012; Chowdhury et al. 2016; Łuczyńska et al. 2018). These factors prompt the research on the removal of metals from water systems.

Several techniques are known for metal ions removal from aqueous solutions, including precipitation (Feng et al. 2000), ion exchange (Hubicki and Kołodyńska 2012), membrane filtration (Chitpong and Husson 2017), and reverse osmosis (Qdais and Moussa 2004). All of them are efficient but very expensive when utilized on a large scale (Fu and Wang 2011; Hashim et al. 2011; Rajasulochana and Preethy 2016). Most cost-effective appears to be adsorption (Bakarat 2011); thus,

✉ Bartosz Mikoda
  bartosz.mikoda@agh.edu.pl

  Agnieszka Gruszecka-Kosowska
  agnieszka.gruszecka@agh.edu.pl

  Agnieszka Klimek
  agaklimek@o2.pl

  Anna Tomczyk
  tomczyk.an@gmail.com

[1] Faculty of Geology, Geophysics and Environmental Protection, AGH University of Science and Technology, al. A. Mickiewicza 30, 30-059 Krakow, Poland

many researchers take great efforts in developing low-cost and environment-friendly adsorbents. Among tested adsorbents, materials derived from organic compounds (Feng et al. 2009, 2010; Senthil Kumar et al. 2012; Lasheen et al. 2012; Taşar et al. 2014), nanoadsorbents (Kyzas and Matis 2015), organic waste (Bożęcka et al. 2016), and mineral adsorbents like raw and synthetic zeolites (Bajda et al. 2004; Choi et al. 2016; Król et al. 2016; Meng et al. 2017) and clay minerals (Srivastava et al. 2005; Doğan et al., 2008; Huang et al. 2015; Yang et al. 2015), clay-bearing mining waste (Helios-Rybicka and Wójcik 2012), dolomite powder (Pehlivan et al. 2009, Gruszecka-Kosowska et al. 2017), calcite sludge (Merrikhpour and Jalali 2012), Ca-Mg phosphate (Ivanets et al. 2017), copper flotation waste (Mikoda et al. 2017), and calcium silicate powder (Ma et al. 2018) were tested in terms of removal of metals from aqueous solutions. It is also advisable that developed adsorbents were easily recoverable. The common practice in regeneration of used adsorbents is washing with different chemicals to obtain "clean" adsorbents. In the study of Li et al. (2016), the modified chitosan has been washed in several cycles with 0.01M EDTA. The outcome of 6 washing cycles was that the adsorption capacity was reduced from 100 to 83%, showing the excellent stability of the adsorbent. The other chemicals used in the regeneration of low-cost adsorbents were alkalized distilled water (pH = 8) for rice husk, which maintained 91% adsorption capacity in the second cycle (Shalaby et al. 2017), and H_2SO_4/NaOH treatment of chitosan, that led to the activation of chitosan, which caused full recovery of adsorption capacity (Schwarz et al. 2018).

Flue gas desulfurization (FGD) gypsum and air pollution control (APC) residues are the types of wastes commonly generated worldwide since virtually every industrial activity producing gas effluents needs to meet air quality standards. FGD residue is a material that is derived from wet flue gas desulfurization processes (Yan et al. 2015). In China, 43 Mt of FGD gypsum was produced in 2010 (Yan et al. 2015), and in Poland, 3 Mt of this waste was generated in 2016 (GUS 2017). The utilization of FGD gypsum is performed, e.g., as set retarder in Portland cement, as road sub-base material or in agricultural purposes (Chandara et al. 2009; Chen et al. 2009; Hua et al. 2010). APC residue in contrary is the material derived from the air pollution control sections in different facilities, such as cyclones or flue gas washing installations (Amutha-Rani et al., 2008). In the world, APC residues are generated in amount of 1.44 Mt annually (Yang et al. 2017). Both types of these wastes are of particular interest because of their fine grain size and high content of heavy metals, which makes their disposal hazardous. Copper industry in Poland is responsible for generating ca 30 Mt of wastes each year, mostly from ore enrichment (Kotarska 2012). The copper smelting facilities produce flue gases that need to be decontaminated before release to the atmosphere; therefore, air pollution control systems and wet flue gas desulfurization are applied to

meet environmental standards. These methods generate ca 214,000 Mg of APC and FGD residues annually in Poland (Górniak-Zimróz 2009). Some of these wastes are utilized as metallurgical flux (ca 20%), and others are landfilled. Thus, the method of utilizing them needs to be developed. The research papers on using of APCR and FGDR as adsorbents in the literature are scarce, the more on their regeneration. The suitability of FGD gypsum as adsorbent of Pb(II) and Cd(II), as well as silicate, selenite, and phosphate ions from both simulated solutions and real wastewater, was previously examined (Bryant et al. 2012; Córdoba et al. 2015; Yan et al. 2015; Kang et al. 2018). The FGD gypsum has been found promising material in metals and anions removal from aqueous solutions. The research on FGD reuse, however, were not carried out by those authors. The FGD gypsum has also been utilized to synthetize hydroxyapatite, which was subsequently tested in metal removal from aqueous solutions with positive results (Yan et al. 2014; Liu et al. 2018).

The aim of this study was to verify the feasibility of air pollution control residues (APCR) and flue gas desulfurization residues (FGDR) from copper foundry in Southwestern Poland as adsorbents of Cu(II) and Pb(II) from simulated aqueous solutions. Sorption capacities with regard to reaction time, initial pH, initial concentration, and adsorbent dose were examined to identify possible mechanisms of adsorption. The experiments were carried out on a pilot scale, since these very materials have not been utilized as adsorbents before. Therefore, the limited amount of experiments has been performed. The further experiments in laboratory scale, as well as semi-industrial scale, are to be undertaken using the input parameters established in this study.

Materials and methods

Material preparation

APCR and FGDR powder samples were received from copper smelter in Głogów (Southwestern Poland), where they were sampled directly from individual places of the process (air pollution control system and wet flue gas desulfurization system, respectively). After transporting to the laboratory, the materials were dried in 70 °C for 24 h using POL-EKO SLN 32 oven. Because of very small grain size (< 0.2 mm), further processing was not required. After such preparation, basic techniques were applied to characterize obtained materials.

Analytical procedures

The chemical composition was determined with the wavelength-dispersive X-ray fluorescence (WDXRF) method, using Rigaku ZSX Primus II apparatus (X-ray tube: end-

window with Rh anode, 4 kW power, 60 kV voltage). Calculations of intensities to obtain the chemical composition were performed using standardless fundamental parameters method (Sherman 1955; Shiraiwa and Fujino 1966). The method used in the calculations is based on the theoretical relations between X-ray intensities and concentrations of elements. No external standards are utilized in the analysis. Instead, the sensitivity library derived with the apparatus, which contains the X-ray intensities on some standards with known elemental composition, is used. In this procedure, the sensitivity library provided by Rigaku has been applied.

Powder X-ray diffraction (XRD) patterns were recorded, using Rigaku MiniFlex 600 apparatus with Cu-Kα radiation, 2–75° 2 range with 0.05° step width. Obtained data were analyzed using XRAYAN software accompanied with JCPDS-ICDD 2013 mineral database.

Infrared (FTIR) spectra of the materials before and after sorption experiments (see the "Sorption experiments" section) were recorded by Bruker Tensor 27 spectrometer using DRIFT technique (3 wt% sample/KBr) in 4000–400 cm^{-1} region at 4 cm^{-1} resolution. Obtained spectra were processed using OMNIC software.

Specific surface area and pore space volume were determined before and after adsorption experiments (see the "Sorption experiments" section), using the N$_2$ adsorption/desorption method in 77 K temperature with Micromeritics ASAP 2020 apparatus. Five-gram portions of APC and FGD residues were heated in 105 °C for 12 h before taking the measurements. The Brunauer-Emmett-Teller (BET) isotherm was used to characterize the specific surface area (S$_{BET}$) of examined materials (Brunauer et al. 1938). The total pore volume was calculated for the relative pressure of $p/p_0 = 0.99$. The volume of micropores ($d < 2$ nm) was calculated, using the Dubinin-Radushkevich method (ISO 15901:3-2007). The volume of mesopores ($2 < d < 50$ nm) was calculated, using the Barrett-Joyner-Halenda (BJH) equation (Barrett et al. 1951). The volume of macropores ($d > 50$ nm) was obtained by subtracting the volumes of micropores and mesopores from the total pore space volume.

The metal concentrations in supernatants after sorption experiments (see the "Sorption experiments" section) were determined by flame atomic absorption spectrometry (FAAS) with Thermo Scientific ICE 3000 Series apparatus using following setup: 0.5-nm spectral slit, 75% lamp current, background correction: off, continuous signal, 0.9–1.1 dm^3 min^{-1} fuel flow. Wave lengths used for analysis were 217 nm for Pb and 324.8 nm for Cu. The limit of quantification was 0.033 µg dm^{-3} for Cu and Pb. The device was calibrated using standard solutions of known Cu and Pb concentrations. The standards were analyzed at least once every ten samples to ensure quality control. Randomly chosen samples were analyzed again to confirm the correctness of measurements.

Preparation of reagents

All chemicals used in this study were of analytical grade (> 99% purity; Chempur, Poland). Stock solutions (10,000 mg dm^{-3}) were prepared by dissolving appropriate amounts of Pb(NO$_3$)$_2$ (CAS: 10099-74-8) and CuSO$_4$ · 5H$_2$O (CAS: 7758-99-8) in de-ionized water (Milli-Q, Millipore). The stock solutions were further dissolved for obtaining binary aqueous solutions of Cu(II) and Pb(II) in five different concentrations: 50, 100, 500, 1000, and 2500 mg dm^{-3} of each metal ion.

Sorption experiments

The sorption experiments were carried out with batch technique. 0.6-g portions of APC and FGD residues were exposed to 30 cm^3 of mixed Cu/Pb solutions. For adsorbent dose test, the same volume of solution was mixed with 0.3, 0.6, and 1.5 g of tested materials (doses of 10, 20, and 50 g dm^{-3}). The effect of pH was examined using aqueous solutions of pH 2–5 for Cu(II) and 2–8 for Pb(II), adjusted with 0.1 M HNO$_3$ and 0.1 M NaOH. The duration of the tests used to investigate the effect of pH was 120 min. The pH ranges for sorption experiments in case of Cu(II) and Pb(II) were different to avoid formation of Cu and Pb hydroxides, which occurs when pH exceeds 5.5 and 8.0 for Cu and Pb, respectively (Ayres et al. 1994). Kinetic studies were carried out using five different contact time periods, i.e., 30, 60, 120, 180, and 240 min. Adsorption isotherms were investigated with five initial concentration values, i.e., 50, 100, 500, 1000, and 2500 mg dm^{-3} for both Cu(II) and Pb(II). Thermodynamics studies were performed in three different temperatures, i.e., 20, 40, and 60 °C. In each experiment, mixtures were shaken at 250 rpm with orbital shaker. After shaking, the solutions were centrifuged, and supernatants were filtered through Whatman® qualitative cellulose filter paper (25-mm diameter, circles). Subsequently, supernatants were acidified to avoid precipitation of metals from solution (Jakimowicz-Hnatyszak and Rubel 1998) and stored in the fridge (4 °C) prior to Cu and Pb analysis (see the "Analytical procedures" section).

Results and discussion

Adsorbent characterization

The XRD analysis (Fig. 1) revealed that the two examined materials differed in mineral composition. The pattern of FGDR sample (Fig. 1(a)) revealed mixed mineral composition of gypsum, hannebachite, calcite, and portlandite. The sole mineral phase observed in APCR sample was gypsum (Fig. 1(b)). Chemical analysis carried out with WDXRF (Table 1) confirmed that chemical composition was in accordance with mineral composition, with CaO and SO$_3$ prevailing in
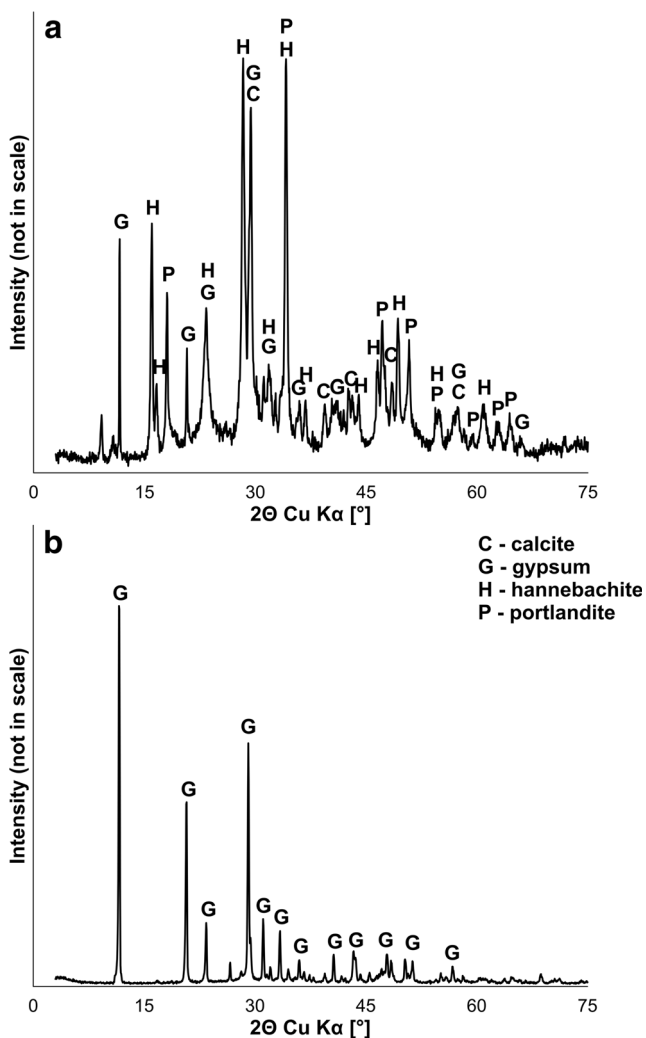
Fig. 1 X-ray diffraction patterns of FGDR (**a**) and APCR (**b**) samples

both material samples (43 and 33.8% respectively for APCR; 54.5 and 37.5% respectively for FGDR). The APCR sample contains substantial amounts of Fe_2O_3, As_2O_3, ZnO, and F (8.24%, 2.94%, 2.28%, and 2.77%, respectively). The total amounts of oxides are not 100% since the elements that were abundant in amount of < 0.1% were not enclosed in Table 1.

The FTIR results for tested adsorbent samples (Fig. 2) were fairly accordant with determined phase composition. In case of APCR before experiments (Fig. 2a), characteristic bands for gypsum (3530, 3400, 1685, 1621, 1116, 668, 601, and

457 cm^{-1}), calcite (872 cm^{-1}), and hannebachite (1475, 1430, and 1108 cm^{-1}) were found. The spectrum of post-adsorption APCR sample (Fig. 2b) was similar, with intensity of some bands reduced. The FGDR sample before experiments spectrum (Fig. 2c) revealed bands characteristic for all minerals determined using XRD (3645 cm^{-1}—portlandite; 3400, 1630, 654, and 490 cm^{-1}—gypsum; 1492, 1475, 1430, 1217, 1108, 984, and 942 cm^{-1}—hannebachite; 2512 and 872 cm^{-1}—calcite). Post-adsorption spectrum for FGDR sample (Fig. 2d) reflected several changes in intensity of bands. The increase was noted for 1430–1492, 1108, and 872 cm^{-1} bands. On the other hand, bands associated with portlandite (3645 cm^{-1}) almost disappeared. However, the shifting of FTIR bands was not observed after the adsorption process, which suggested that the process did not cause the formation of additional metal-ion associations and had no influence on the structure of the adsorbent.

The textural parameters (Table 2) reflected the feasibility of utilizing tested materials as adsorbents. Both materials were characterized by relatively high specific surface area (66.8 and 28.8 m^2 g^{-1} for APCR and FGDR, respectively) when compared to other waste materials from copper enrichment facilities (copper flotation waste—6.24 m^2 g^{-1}) (Mikoda and Gruszecka-Kosowska 2018); however, the surface area is low when compared to other efficient adsorbents such as activated carbon or natural bentonite (1239 and 1000 m^2 g^{-1}, respectively) (Patnukao et al. 2008; Iskander et al. 2011). Low pore space volume (0.158 and 0.142 cm^3 g^{-1} for APCR and FGDR, respectively) is common for microporous materials. However, as per pores dimension, mesopores dominated in APCR sample, while meso- and macropores were prevailing in FGDR sample. After the experiments, samples exhibited slightly different properties. In case of APCR, a decrease of surface area was observed along with the decrease of mesopores percentage and increase of macropores volume, which implied that the mesopores could be occupied by adsorbed ions. The surface area of FGDR sample also slightly decreased, but in this case, the volume of mesopores increased at the expense of macropores, suggesting that adsorbed particles could occupy mesopores. The analysis of N_2 adsorption/desorption isotherms (Fig. 3) revealed that in case of both adsorbents, the isotherms exhibited type IV of adsorption isotherm and H3 hysteresis loop, that are typical for mesoporous and slit-shape pored materials (Sing et al. 1985).

Table 1 Chemical (oxide) composition of APCR and FGDR samples determined by WDXRF (all results in wt%)

Sample	CaO	SiO₂	Al₂O₃	K₂O	Na₂O	MgO	Fe₂O₃	SO₃	CuO	PbO	As₂O₃	ZnO	F	Cl	Total
APCR	43.0	2.97	0.56	0.11	0.54	1.02	8.24	33.8	0.29	0.73	2.94	2.28	2.77	0.15	99.40
FGDR	54.5	1.45	0.41	0.13	0.25	1.09	1.92	37.5	0.33	0.29	0.63	n.d.	0.84	99.77

n.d. not detected

Fig. 2 FTIR spectra of APCR sample before and after adsorption (**a**) and FGDR sample before and after adsorption (**b**)

APCR before adsorption
APCR after adsorption
FGDR before adsorption
FGDR after adsorption
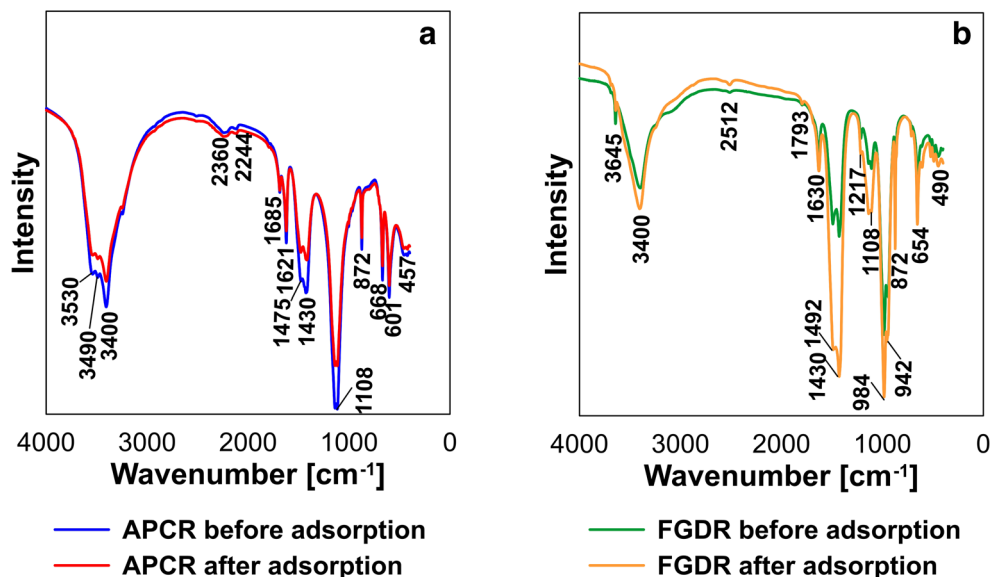
Effect of pH

The pH value is defined as one of the most important factors affecting the adsorption process due to its influence on speciation of metals and the surface properties of the adsorbent (Mohammadi et al. 2015; Yan et al. 2015). In this study, pH ranging from 2 to 5 was used for Cu(II) and from 2 to 8 range was applied for Pb(II) (see the "Sorption experiments" section). The pH value was surprisingly found as not governing the adsorption of metals on APCR and FGDR samples (Fig. 4), while other studies show dependence of adsorption on pH (e.g., Yan et al. 2015; Mikoda et al. 2017; Gruszecka-Kosowska et al. 2017). The sorption values maintained at about 78 mmol kg^{-1} Cu(II) and about 24 mmol kg^{-1} Pb(II) for both analyzed material samples at initial concentration of Pb and Cu equal to 100 mg dm^{-3}. For that reason, other experiments were conducted at initial pH 3.0 (acidic), because this value is below the hydroxide formation point for both ions, which should secure the metals dissolved in the solution. Thus, research in real effluent will be performed in higher pH values. Before, repetition of the experiment on pilot scale will be made to investigate the reason of metals adsorption being not dependent on initial pH values.

Effect of adsorbent dose

Both examined ions exhibited similar behavior in relation to adsorbent dose (Fig. 5). The amount of adsorbed Cu(II) and Pb(II) decreased rapidly (exponentially) with increasing adsorbent dose. The biggest leap was noted between 10 and 20 g dm^{-3} doses, where amounts of adsorbed ions decreased twofold. For Cu(II), this decrease tempo was maintained with increasing dose (20 to 50 g dm^{-3}), whereas for Pb(II), it even increased to threefold. Namasivayam and Kumuthu (1998) stated that this phenomenon might be due to "over-crowding" of adsorbent particles, which means that there is "too much" adsorbent to the extent that the process is stopped. The results showed that assumed absorbent doses were too high. This part of experiments will be repeated before industrial scale research; however, it seems that low doses of adsorbent should be effective in Pb and Cu removal. It means that relatively low amounts of material would be enough for wastewater purification. This might reduce the additional waste generation in case if adsorbent regeneration would be technically not possible or economically unprofitable.

Table 2 Textural parameters of APCR and FGDR samples before and after adsorption

Sample		Specific surface area S_{BET} [m^2 g^{-1}]	Total pore volume [cm^3 g^{-1}]	Pore fractions in total pore volume [%]		
				Micropores	Mesopores	Macropores
Before	APCR	66.8	0.158	14.6	70.8	14.6
	FGDR	28.8	0.142	7.0	46.5	46.5
After	APCR	65.5	0.159	14.5	66.0	19.5
	FGDR	24.7	0.121	7.4	57.9	34.7

Fig. 3 The N$_2$ adsorption/desorption isotherms for APCR and FGDR samples
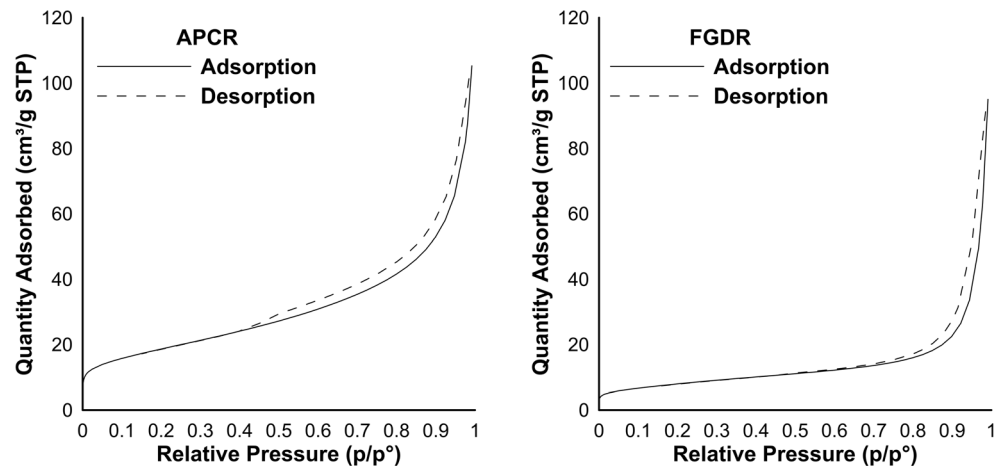
Equilibrium sorption modeling

Modeling of adsorption can be performed in different ways. Most popular method is describing the process using isotherms, being the relation of amount of metal adsorbed as a function of equilibrium concentration at the same temperature. The isotherms are useful in understanding the mechanism of adsorption and in designing optimal process conditions (Matusik 2014; Mohammadi et al. 2015; Yan et al. 2015). Freundlich, Langmuir, and Dubinin-Radushkevich (D-R) models (Eqs. 1–3) are often used and well described in literature.

Freundlich model is based on the assumption that the adsorption process is infinite and the surface of the adsorbent is heterogenous. This equation is purely theory-based, since the saturation phenomena occur in actual solid/liquid mixtures (Król et al. 2016).

On the other hand, Langmuir theory applies to homogenous adsorbent surfaces. The model assumes that there is no interaction between adsorbed molecules and that the particles are bonded with the same mechanism and activation energy. The process is limited in this model by the number of active sites, leading to creation of a single layer of molecules on the adsorbent's surface (Yan et al. 2014; Maziarz and Matusik 2016).

The D-R model gives a basic idea about the mechanism of adsorption, which is not given by Langmuir or Freundlich equations. The parameters of the model help to verify whether the adsorption is of physical or chemical nature; the determination is based on the mean adsorption energy (E) [kJ mol^{-1}]; if $E < 8$, the process is of physical nature; if $8 < E < 16$, the adsorption takes place via ion exchange; if $E > 16$, then the process is of chemical nature (Yan et al. 2015).

In this study, Freundlich, Langmuir, and Dubinin-Radushkevich (D-R) models were used. For the Freundlich model of sorption, formula (1) (Freundlich 1906) was applied. For the Langmuir model of sorption, formula (2) (Langmuir 1918) was used. For D-R isotherm, formula (3) (Dubinin et al. 1949) was applied:

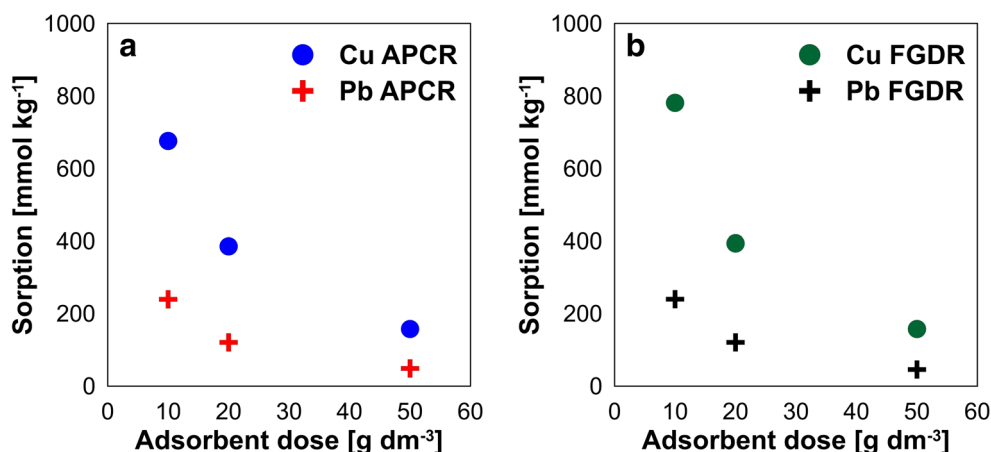$$q_{eq} = K_F C_{eq}^{1/n} \tag{1}$$

$$q_{eq} = \frac{K_L q_m C_{eq}}{1 + K_L C_{eq}} \tag{2}$$

$$\ln q_{eq} = \ln q_m - \beta \varepsilon^2 \tag{3}$$

Fig. 4 Effect of pH on adsorption of metal ions onto APCR (a) and FGDR (b) samples
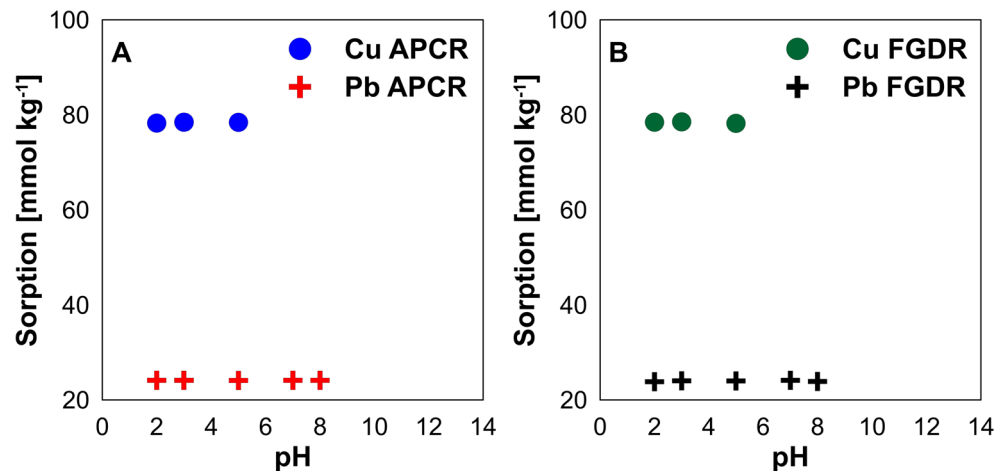
Fig. 5 Effect of adsorbent concentration on adsorption of metal ions onto APCR (**a**) and FGDR (**b**) samples

where q_{eq} is the sorption capacity at equilibrium [mmol kg^{-1}], C_{eq} is the equilibrium concentration [mmol dm^{-3}], K_L is the Langmuir adsorption constant [dm^3 mmol^{-1}], q_m is the maximum adsorption capacity [mmol kg^{-1}], K_F is the Freundlich adsorption capacity [mmol kg^{-1}], n is the Freundlich dimensionless constant, β is the D-R constant [mol^2 J^{-2}], and ε is the Polanyi potential (Eq. 4):

$$\varepsilon = RT\ln\left(1 + \frac{1}{C_{eq}}\right) \tag{4}$$

where R is the gas constant (8.31446 J mol^{-1} K^{-1}), T is the absolute temperature [K], and C_{eq} is the equilibrium concentration [mmol dm^{-3}].

The mean adsorption energy was calculated with the following formula (5):

$$E = \frac{1}{\sqrt{-2\beta}} \tag{5}$$

where E is the mean adsorption energy [kJ mol^{-1}] and β is the D-R constant [mol^2 J^{-2}].

The isotherms along with Langmuir, Freundlich, and Dubinin-Radushkevich model values were shown on Fig. 6a–f. The isotherm parameters and constants shown in Table 3 revealed that the data for Pb(II) (Fig. 6b) and Cu(II) (Fig. 6a) adsorbed on FGDR sample followed the Langmuir model; Cu(II) data followed the model very well ($R^2 = 0.99$). The model was found to illustrate moderately the Pb(II) adsorption data onto FGDR ($R^2 = 0.90$). The Langmuir model was perfectly fitted also for Cu(II) sorption onto APCR sample (Fig. 6a; $R^2 = 1$). For Pb(II) adsorption on FGDR, Freundlich equation gave much better correlation ($R^2 = 0.84$) than of Langmuir model ($R^2 = 0.05$); however, both R^2 values show that this model is not good for displaying the Pb(II) adsorption onto FGDR (Fig. 6c, d).

The Dubinin-Radushkevich model (Fig. 6e, f) was found to be moderately fitted to Cu(II) adsorption data onto both adsorbents (R^2 equal to 0.96 and 0.95 for APCR and FGDR, respectively) and not fitting the Pb(II) adsorption data for both materials (0.81 and 0.07 R^2 values for APCR and FGDR, respectively). The maximum adsorption capacities of Cu(II) were 676.0 mmol kg^{-1} for APCR and 1554 mmol kg^{-1} for FGDR, which after calculation were equal to 42.9 and 98.8 mg g^{-1}, respectively. In case of Pb(II), the capacities were 600.6 mmol kg^{-1} for APCR and 602 mmol kg^{-1} for FGDR (124.4 and 124.7 mg g^{-1} respectively after calculation). Langmuir model capacities q_m for Cu(II) were fairly accordant with obtained real data (588 and 1667 mmol kg^{-1} for APCR and FGDR, respectively), and far better than Freundlich K_F constants (302 and 849 mmol kg^{-1} for APCR and FGDR, respectively). On the other hand, Freundlich (K_F; 4540 and 310 mmol kg^{-1} for APCR and FGDR, respectively) and Langmuir (q_m; 1111 and 200 mmol kg^{-1} for APCR and FGDR, respectively) model capacities for Pb(II) are strongly inadequate, even when fairly good correlation was found. Good accordance of data with Langmuir model may suggest that the process was unidirectional (Merrikhpour and Jalali 2012). The Langmuir constant b was used to calculate dimensionless separation factor ($R_L = (1 + bC_0)^{-1}$; C_0—initial concentration [mg dm^{-3}]) that is used to assess the favorability of adsorption (Yan et al. 2015). The results were shown on Fig. 7a for APCR and Fig. 7b for FGDR as function of R_L against C_0. All R_L values fell into 0–1 range, which implied that the adsorption was favorable (Meitei and Prasad 2014). Moreover, the R_L values from Fig. 7 were mostly higher for Pb(II) than for Cu(II), suggesting higher affinity between Pb(II) and both adsorbents. Similar results were obtained by Yan et al. (2014, 2015) using FGD gypsum to remove Pb(II) ions from aqueous solutions. The explanation of this phenomenon can be as follows: (i) the smaller hydrated radius of Pb(II) (0.261 nm) than of Cu(II) (0.295 nm), that
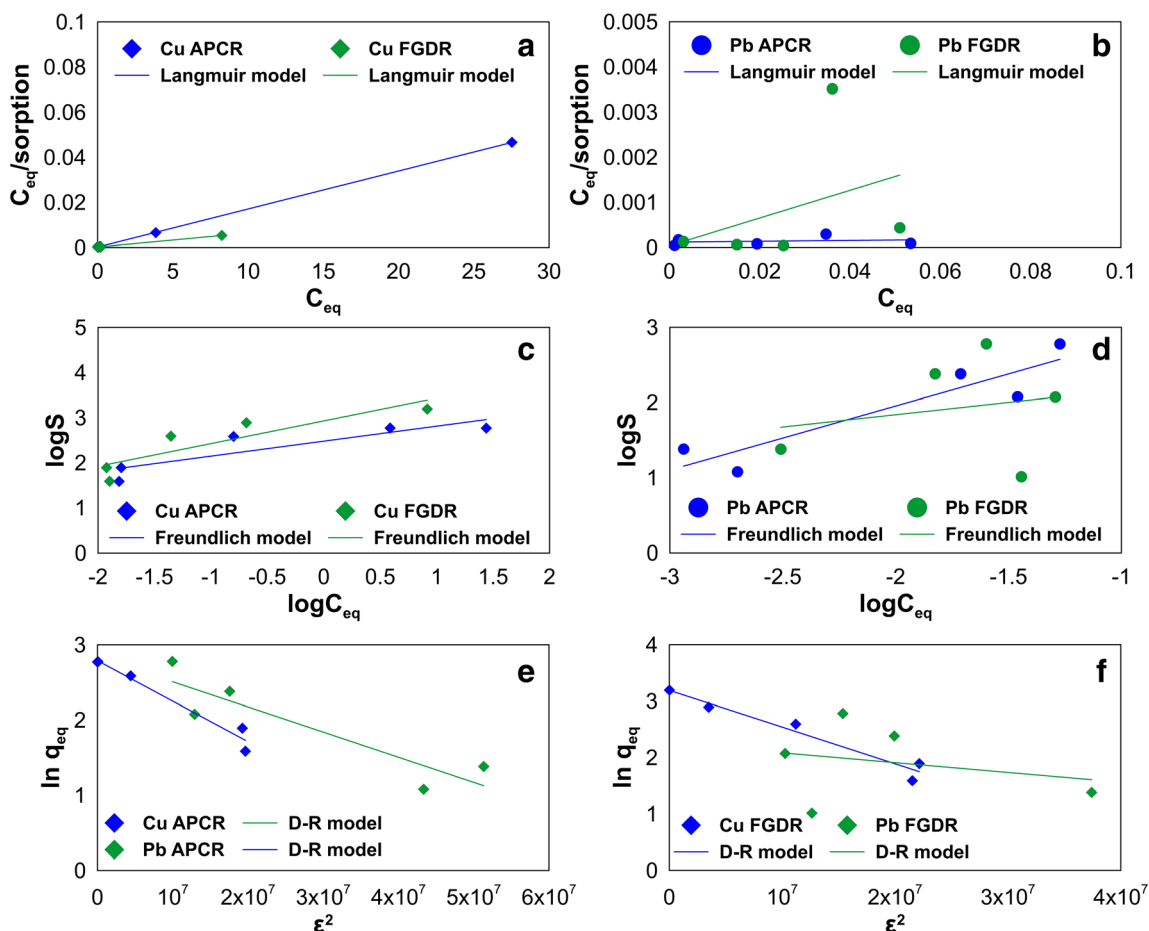
Fig. 6 Langmuir, Freundlich, and Dubinin-Radushkevich (D-R) isotherm plots for the adsorption of Cu(II) onto APCR (**a**), Pb(II) onto APCR (**b**), Cu(II) onto FGDR (**c**), Pb(II) onto FGDR (**d**), Cu(II) and Pb(II) onto APCR (**e**), and Cu(II) and Pb(II) onto FGDR (**f**)

can suggest higher accessibility of Pb(II) for FGDR and APCR; (ii) higher electronegativity of Pb(II) (2.33) than of Cu(II) (1.90), that suggests stronger attraction of Pb(II) to the surface of the adsorbents; (iii) the ionic radius of Pb(II) (0.122 nm) is larger than of Ca(II) (0.097 nm), while that of Cu(II) (0.072 nm) is smaller than that of Ca(II), which suggests that Cu(II) is less likely to be incorporated to the structure of APCR and FGDR (Yan et al. 2014, 2015). The favorability of adsorption can also be assessed

with Freundlich's model exponent (*n*). Values of $1/n$ (Table 3) fell into 0–1 range for both adsorbents and both ions, indicating favorable adsorption of Cu and Pb onto APCR and FGDR. Also, the K_F constant gives some information about binding affinity of ions (Ma et al. 2011). In case of APCR, the K_F value for Pb(II) was higher, implying stronger affinity of Pb(II) to APCR. This finding was compliant with comparison of R_L values from Fig. 6. On the other hand, K_F values for FGDR suggest that Cu(II) was bonded stronger to the

Table 3 Langmuir, Freundlich, and Dubinin-Radushkevich constants and correlation coefficients for adsorption of metal ions onto APCR and FGDR samples

Sample	Metal	Langmuir model			Freundlich model			Dubinin-Radushkevich model		
		q_m [mmol kg^{-1}]	K_L [dm^3 mmol^{-1}]	R^2 [–]	$1/n$ [–]	K_F [mmol kg^{-1}]	R^2 [–]	β [mol^2 J^{-2}]	E [kJ mol^{-1}]	R^2 [–]
APCR	Cu(II)	588	8.50	1.00	0.33	302	0.77	4.23E−08	3.44	0.96
	Pb(II)	1111	9.00	0.05	0.85	4540	0.84	2.26E−08	4.70	0.81
FGDR	Cu(II)	1667	3.00	0.99	0.50	849	0.78	5.35E−08	3.06	0.95
	Pb(II)	200	100	0.90	0.33	310	0.05	2.00E−08	5.00	0.07

Fig. 7 Separation factor, R_L, for the adsorption of Pb(II) and Cu(II) at different initial concentrations (C_0) onto APCR (A) and FGDR (A) samples
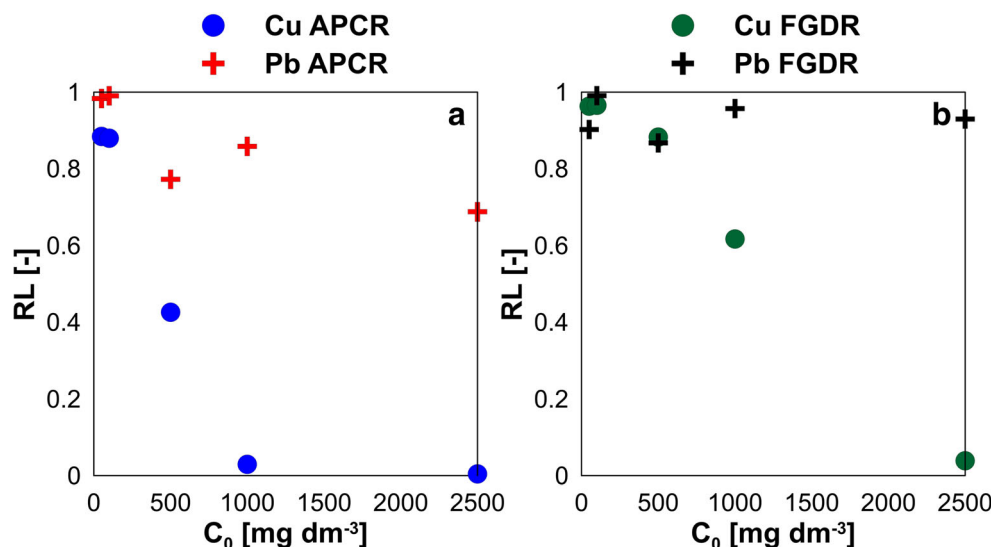
adsorbent, contrary to R_L results and results obtained by Yan et al. (2015).

The data for D-R model (Table 3) suggested that the mean adsorption energy (E) fell into 3–5 kJ mol^{-1} range for all samples. The E values were below 8 kJ mol^{-1}, so the adsorption presumably was of physical nature and metals were weakly bonded with the adsorbent, which again was contrary to results of Yan et al. (2015). The reason of these differences might be due to different mineral composition (relatively pure FGD gypsum versus mixed calcium sulfate-carbonate-hydroxide FGDR sample).

Thermodynamic studies were conducted in 20, 40, and 60 °C. The input parameters were 500 mg dm^{-3} initial metal concentration, pH 3.0, 60-min reaction time. The Gibbs free energy change ($\Delta G°$, kJ mol^{-1}), enthalpy change ($\Delta H°$, kJ mol^{-1}), and entropy change ($\Delta S°$, kJ mol^{-1} K^{-1}) were calculated using van't Hoff's equations (Eqs. 6–8; Milonjić 2007; Yan et al. 2015; Frantz et al. 2017):

$$K = \frac{C_s}{C_{eq}} \tag{6}$$

$$\Delta G° = R_T \ln K \tag{7}$$

$$\ln K = \frac{\Delta S°}{R} - \frac{\Delta H°}{RT} \tag{8}$$

where K is the dimensionless adsorption equilibrium constant, R is the gas constant (8.31446 J mol^{-1} K^{-1}), T is the absolute temperature [K], C_s is the equilibrium sorption capacity [mmol dm^{-3}], and C_{eq} is the equilibrium concentration [mmol dm^{-3}].

As shown in Table 4, $\Delta G°$ absolute values for Cu(II) adsorption onto APCR decreased with temperature rising, suggesting that lower temperature favored the process. On the

other hand, $\Delta G°$ absolute values for APCR were increasing for Pb(II) adsorption with the temperature increase, implying different behavior of this ion in thermodynamic context. The $\Delta G°$ absolute values for adsorption of ions onto FGDR were in indirect proportion with the temperature for both Cu(II) and Pb(II), which implied that lower temperature was favoring the adsorption process as well. Generally, lower temperature was more advantageous for adsorption on both materials. Negative $\Delta G°$ and positive $\Delta H°$ values for Cu(II) adsorption onto both adsorbents indicated that the process was spontaneous and endothermic. On the other hand, $\Delta G°$ values for Pb(II) adsorption onto both adsorbents were positive and $\Delta H°$ values were negative, suggesting not spontaneous and exothermic adsorption process. Enthalpy change $\Delta H°$ is used as an indicator of sorption mechanism (2.1–20.9 kJ mol^{-1}—physisorption; 20.9–418.4 kJ mol^{-1}—chemisorption) (Sağ and Kutsal 2000). In case of both investigated adsorbent samples and Cu(II) ion, the values of enthalpy change exceeded 20.9 kJ mol^{-1}, which implied that the process was of chemical nature. On the other hand, the absolute enthalpy change values for Pb(II) adsorption onto both adsorbents fell into 2.1–20.9 kJ mol^{-1} range, which suggest the physisorption as the prevailing mechanism. Positive values of $\Delta S°$ for Cu(II) adsorption onto both adsorbents implicated the increase of randomness of solid-liquid interface, which aided the adsorption process.

Sorption kinetics

The kinetics of adsorption process is of great importance in terms of technological optimization of the process efficiency (Mohammadi et al. 2015). Figure 8 shows that the equilibrium was reached at 30 min of reaction time; thus, in case of materials used, the contact time could be shorter. The rapid

Table 4 Thermodynamic parameters for metal ions adsorption onto APCR and FGDR samples

Sample	Metal	T (°C)	Sorption (mmol dm^{-3})	ΔG (kJ mol^{-1})	ΔH (kJ mol^{-1})	ΔS (kJ mol^{-1} K^{-1})
APCR	Cu(II)	20	7.83	− 1.28		
		40	7.81	− 0.88	32.5	0.11
		60	7.77	− 0.30		
	Pb(II)	20	2.40	0.07		
		40	2.39	0.61	− 10.6	− 0.11
		60	2.37	1.54		
FGDR	Cu(II)	20	7.85	− 2.14		
		40	7.79	− 0.52	39.6	0.13
		60	7.84	− 1.88		
	Pb(II)	20	2.40	− 0.08		
		40	2.34	2.04	− 30.8	− 0.31
		60	2.40	− 0.04		

adsorption of metal ions and silicate anions has been proved for FGD gypsum in the studies of other authors (Yan et al. 2015; Kang et al. 2018). This finding is essential for industrial practices, since shorter contact time ensures lower costs for the removal process, which is a strong point in using those materials in real wastewater treatment. The most commonly used models are pseudo-first-order model, described by the equation (Eq. 9) and pseudo-second-order model, described by the equation (Eq. 10) (Matusik 2014):

$$\log\left(q_{eq} - q_t\right) = \log q_{eq} - \frac{k_1 t}{2.303} \tag{9}$$

$$\frac{t}{q_t} = \frac{1}{k_2 q_{eq}^2} + \frac{t}{q_{eq}} \tag{10}$$

where q_{eq} is the sorption capacity at equilibrium [mmol kg^{-1}], q_t is the sorption capacity at time t [mmol kg^{-1}], k_1 is the first-order rate constant [min^{-1}], and k_2 is the second-order rate constant [kg mmol^{-1} min^{-1}].

The constants and correlation coefficients of kinetic models (Table 5) showed that Cu(II) and Pb(II) adsorption on APCR and FGDR was perfectly fitted to pseudo-second-order equation ($R^2 = 1$), which was also illustrated on Fig. 9(b). Some authors (Ho and McKay 1998; Merrikhpour and Jalali 2012; Cherifi et al. 2013) imply that the fact that the experimental data were perfectly expressed by pseudo-second-order model could be a sign of chemical adsorption as prevailing in the process. These statements, however, are contradictory to E values (Table 3) as indicators of physical nature of the process; therefore, the authors believe that chemisorption is out of question as possible adsorption mechanism for Cu(II) and Pb(II) onto APCR and FGDR.

Research perspectives

The preliminary research conducted in a batch mode and laboratory scale showed that APCR and FGDR are promising

**Fig. 8** Effect of contact time on adsorption of metal ions onto APCR (**a**) and FGDR (**b**) samples
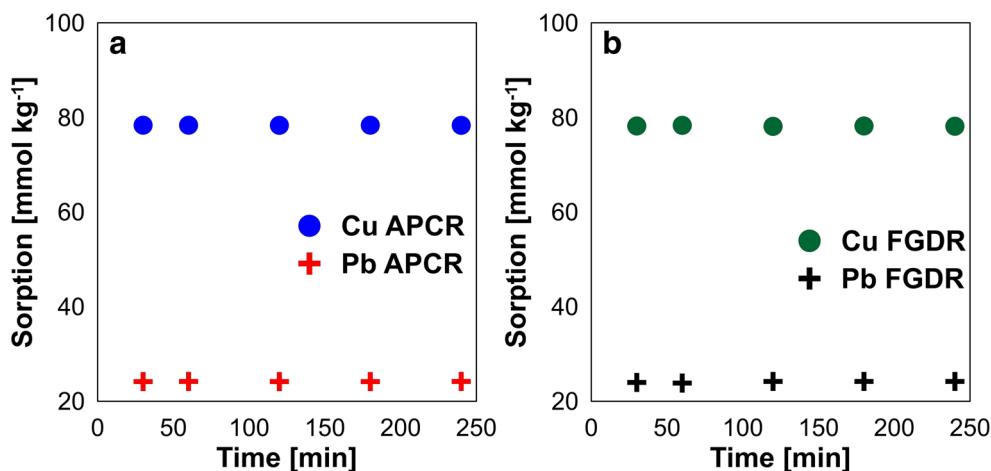
Table 5 Correlation coefficients and adsorption rate constants for kinetic models of metal ions adsorption onto APCR and FGDR samples

Sample	Metal	Pseudo-first-order model		Pseudo-second-order model	
		R^2 [−]	k_1 [min^{-1}]	R^2 [−]	k_2 [kg mmol^{-1} min^{-1}]
APCR	Cu(II)	0.04	0.045	1.00	0.232
	Pb(II)	0.35	0.024	1.00	0.058
FGDR	Cu(II)	0.27	0.034	1.00	0.032
	Pb(II)	0.65	0.049	1.00	0.121

materials to be considered as adsorbents in heavy metal removal from aqueous solutions. The results were unusual at some points. For instance, the pH of the solution and the reaction time were found to not govern the adsorption process, which is contrary to other works describing the metal removal

by low-cost adsorbents (e.g., Yan et al. 2015). The pilot-scale research was designed to prove the feasibility of the waste materials for metal removal. The drawbacks recorded during the experiments will be eliminated by repetition of research with inadequate results. Secondly, the adsorbent doses used in this study appear to be too high, since only in case of Cu(II) for APCR, the 100% adsorption capacity has been reached, while in case of other ions, the capacity reached 30–50% when the 10 g dm^{-3} dose has been applied. Therefore, the repetition of experiments using much lower doses is also planned. Encouraging is the fact that lower adsorbent doses indicate the low amounts of adsorbent needed to clean a wastewater in industrial scale process. The obvious next step is using the tested adsorbents in fixed bed adsorption column experiments. The fixed bed adsorption is far more realistic in industrial practice since large streams of wastewater are generated in manufactures, and the batch mode is more efficient for certain effluent concentrations (Dichiara et al. 2015); it is

Fig. 9 Pseudo-first-order (**a**) and pseudo-second-order (**b**) kinetic models of adsorption of metal ions onto APCR and FGDR samples
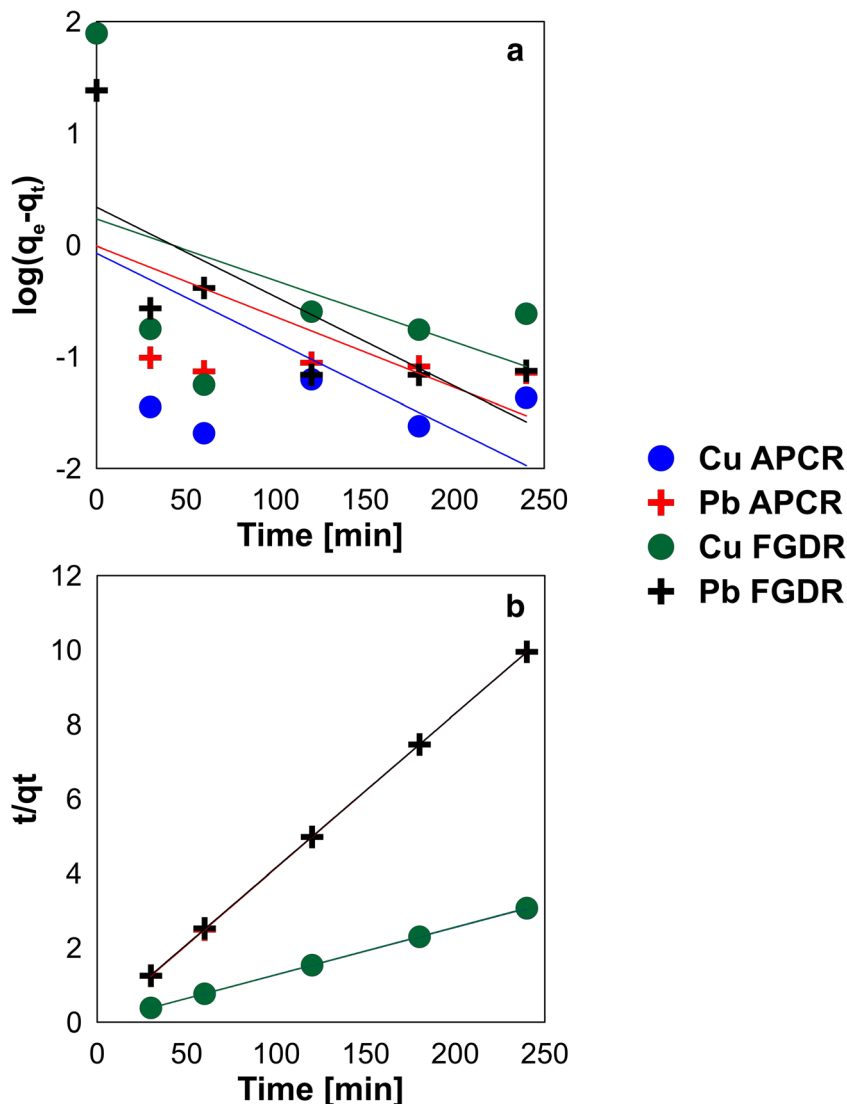
Table 6 Comparison of adsorption capacity for heavy metal ions of APCR and FGDR with other adsorbents

Metals	Adsorbent	Adsorption capacity [mg g^{-1}]	Reference
Cu(II), Pb(II)	APCR	42.9, 124.4	This paper
Cu(II), Pb(II)	FGDR	98.8, 124.7	This paper
Cu(II), Pb(II)	Waste calcite sludge	1067.8, 534.2	Merrikhpour and Jalali 2012
Cu(II), Pb(II)	Copper flotation waste	58.8, 83.3	Mikoda et al. 2017
Cu(II), Pb(II)	Bog iron ore	25.2, 97.0	Rzepa et al. 2009
Cu(II), Pb(II)	Ca-Mg phosphate	240.2, 246.6	Ivanets et al. 2017
Cu(II), Pb(II)	Zeolite	10.9, 28.3	Bajda et al. 2004
Cu(II), Pb(II)	Zeolite A	62.4, 227.7	Meng et al. 2017
Cu(II), Pb(II)	Mg-zeolite	15.2, 58.5	Choi et al. 2016
Cu(II)	Calcium silicate powder	680.9	Ma et al. 2018
Pb(II)	FGD gypsum	161.3	Yan et al. 2015
Cu(II), Pb(II)	Dolomite powder	8.26, 21.7	Pehlivan et al. 2009
Pb(II)	Colemanite ore waste	33.6	Sari and Tuzen 2009
Pb(II)	Jordanian sorbent	66.3	Al-Degs et al. 2006
Pb(II)	Synthetic hydroxyapatite	277.8	Yan et al. 2014

not designed to recover the industrially generated amounts of wastewater (Unuabonah et al. 2010). The information obtained during the fixed bed column experiments is helpful in designing the real-case scenario that gives proper characteristic of tested adsorbent in terms of its potential in purification of industrial effluents and verifies the feasibility of the material to be utilized in a large-scale wastewater treatment.

Comparison of adsorption capacity of examined materials with other mineral adsorbents

The results of adsorption capacity for APCR and FGDR from copper foundry in Southwestern Poland were compared to low-cost mineral adsorbents analyzed in other research (Table 6). The literature research showed that the Cu(II) capacity of APCR was higher than that of dolomite powder (8.26 mg g^{-1}), zeolite (10.9 mg g^{-1}), Mg-zeolite (15.2 mg g^{-1}), and bog iron ore (25.2 mg g^{-1}) and lower than that of copper flotation waste (58.8 mg g^{-1}), zeolite A (62.4 mg g^{-1}), FGDR (98.8 mg g^{-1}), Ca-Mg phosphate (240.2 mg g^{-1}), calcium silicate powder (680.9 mg g^{-1}), and waste calcite sludge (1067.2 mg g^{-1}). The capacities of both adsorbents analyzed in this study for Pb(II) (since they are virtually the same) were found to be higher than that of dolomite powder (21.7 mg g^{-1}), zeolite (28.3 mg g^{-1}), colemanite ore waste (33.6 mg g^{-1}), Mg-zeolite (58.5 mg g^{-1}), Jordanian sorbent (66.3 mg g^{-1}), copper flotation waste (83.3 mg g^{-1}), and bog iron ore (97 mg g^{-1}) and lower than that of FGD gypsum (161.3 mg g^{-1}), zeolite A (227.7 mg g^{-1}), Ca-Mg phosphate (246.6 mg g^{-1}), synthetic hydroxyapatite (277.8 mg g^{-1}), and waste calcite sludge (534.2 mg g^{-1}). The study revealed that APCR and FGDR samples were competitive as adsorbents of Cu(II) and Pb(II) from aqueous solutions when compared to other low-cost adsorbents. Presumably, the materials will also be competitive to other materials taking under consideration contact time of the adsorption process and adsorbent dose used for removal of metals from aqueous solutions.

Conclusions

This work was aimed at the evaluation of APC and FGD residues from copper foundry in Southwestern Poland for heavy metal removal from simulated binary aqueous solutions with help of batch experiments using various input parameters. Conclusions that can be drawn from this study are the following:

a. The residues from air pollution control (APCR) and flue gas desulfurization (FGDR) from copper smelting facility could be considered as adsorbents of heavy metals from aqueous solutions.
b. The adsorption process on APCR and FGDR samples was not dependent on time and pH values in the tested range, which was in opposition to data for other adsorption materials.
c. The increase of adsorbent dose suppressed the adsorption process in the tested range. Thus, lower doses of the adsorbent will be used in further research and lower amounts of material would be used in comparison to other materials.
d. Equilibrium studies revealed that adsorption data followed Langmuir model quite well, except for Pb(II) adsorption on FGDR, which did not follow any of the models. The mean adsorption energy suggested that the process took place as a physisorption.

e. Sorption kinetics of both Cu(II) and Pb(II) on both materials was expressed perfectly ($R^2 = 1$) using pseudo-second-order equation.

f. Thermodynamic studies showed that the process was spontaneous and endothermic for Cu(II) and not spontaneous and exothermic and Pb(II). Lower temperature was found more appropriate for the adsorption.

g. The maximum sorption capacities of both materials were equal to 42.9 mg g^{-1} Cu(II) and 124.4 mg g^{-1} Pb(II) for APCR and 98.8 mg g^{-1} Cu(II) and 124.7 mg g^{-1} Pb(II) for FGDR, which was comparable to other low-cost adsorbents.

References

Adriano DC (2001) Trace elements in terrestrial environments: biogeochemistry, bioavailability, and risks of metals. Springer, New York

Al-Degs Y, El-Barghouthi MI, Issa AA, Khraisheh MA, Walker GM (2006) Sorption of Zn(II), Pb(II) and Co(II) using natural sorbents: equilibrium and kinetic studies. Water Res 40:2645–2658

Amutha-Rani D, Boccaccini AR, Deegan D, Cheeseman CR (2008) Air pollution control residues from waste incineration: current UK situation and assessment of alternative technologies. Waste Manag 28(11):2279–2292

Ayres DM, Davis AP, Gietka PM (1994) Removing heavy metals from wastewater. Engineering research center report, University of Maryland

Bajda T, Franus W, Manecki A, Manecki M, Mozgawa W, Sikora M (2004) Sorption of heavy metals on natural zeolite and smectite-zeolite shale from the Polish Flysch Carpathians. Pol J Environ Stud 13:7–10

Bakarat MA (2011) New trends in removing heavy metals from industrial wastewater. Arab J Chem 4(4):361–377

Barrett EP, Joyner LG, Halenda PP (1951) The determination of pore volume and area distributions in porous substances. I Computations from Nitrogen Isotherms. J Am Chem Soc 73(1): 373–380

Bożęcka A, Bożęcki P, Sanak-Rydlewska S (2016) Removal of Pb(II) and Cd(II) ions from aqueous solutions with selected organic wastes. Physicochem Probl Mi 52(1):380–396

Brunauer S, Emmett PH, Teller E (1938) Adsorption of gases in multi-molecular layers. J Am Chem Soc 60(2):309–319

Bryant RB, Buda AR, Kleinman PJ, Church CD, Saporito LS, Folmar GJ, Bose S, Allen AL (2012) Using flue gas desulfurization gypsum to remove dissolved phosphorus from agricultural drainage waters. J Environ Qual 41(3):664–671

Chandara C, Azizli KAM, Ahmad ZA, Sakai E (2009) Use of waste gypsum to replace natural gypsum as set retarders in Portland cement. Waste Manag 29(5):1675–1679

Chen L, Ramsier C, Bigham J, Slater B, Kost D, Lee YB, Dick WA (2009) Oxidation of FGD-CaSO$_3$ and effect on soil chemical properties when applied to the soil surface. Fuel 88(7):1167–1172

Cherifi H, Fatiha B, Salah H (2013) Kinetic studies on the adsorption of methylene blue onto vegetal fiber activated carbons. Appl Surf Sci 282:52–59

Chitpong N, Husson SM (2017) Polyacid functionalized cellulose nano-fiber membranes for removal of heavy metals from impaired waters. J Membr Sci 523:418–429

Choi H-J, Yu S-W, Kim KH (2016) Efficient use of Mg-modified zeolite in the treatment of aqueous solution contaminated with heavy metal toxic ions. J Taiwan Inst Chem Eng 63:482–489

Chowdhury S, Jafar Mazumder MA, Al-Attas O, Husain T (2016) Heavy metals in drinking water: occurrences, implications, and future needs in developing countries. Sci Total Environ 569–570:476–488

Córdoba P, González ME, González A, Maroto-Valer M, Moreno N, Sepúlveda N, Navia R, Querol X (2015) Evaluation of a flue gas desulphurisation (FGD)-gypsum from a wet limestone FGD as adsorbent for removal of selenium in water streams. J Environ Anal Toxicol 5(5):305. https://doi.org/10.4172/2161-0525.1000305

Dichiara AB, Weinstein SJ, Rogers RE (2015) On the choice of batch or fixed bed adsorption processes for wastewater treatment. Ind Eng Chem Res 54(34):8579–8586

Doğan M, Turhan Y, Alkan M, Namli H, Turan P, Demirbaş Ö (2008) Functionalized sepiolite for heavy metal ions adsorption. Desalination 230(1–3):248–268

Dubinin MM, Zaverina ED, Radushkevich LV (1949) Sorption and structure of active carbons. I. Adsorption of organic vapors. Russ J Phys Chem A 21:1351–1362

Feng D, Aldrich C, Tan H (2000) Treatment of acid mine water by use of heavy metal precipitation and ion exchange. Miner Eng 13(6):623–642

Feng N, Guo X, Liang S (2009) Adsorption study of copper (II) by chemically modified orange peel. J Hazard Mater 164:1286–1292

Feng N, Guo X, Liang S (2010) Enhanced Cu(II) adsorption by orange peel modified with sodium hydroxide. Trans Nonferrous Metals Soc China 20:146–152

Frantz TS, Silveira N Jr, Quadro MS, Andreazza R, Barcelos AA, Cadaval TSS Jr, Pinto LAA (2017) Cu(II) adsorption from copper mine water by chitosan films and the matrix effects. Environ Sci Pollut Res 24:5908–5917

Freundlich HMF (1906) Uber die Adsorption in Lösungen. Z Phys Chem 57A:385–470

Fu F, Wang Q (2011) Removal of heavy metal ions from wastewaters: a review. J Environ Manag 92:407–418

Górniak-Zimróz J (2009) Źródła i koszty środowiskowe gospodarki odpadami w KGHM Polska Miedź S.A. Prace Naukowe Instytutu Górnictwa Politechniki Wrocławskiej 128(36):103–116 (in Polish)

Gruszecka-Kosowska A, Baran P, Wdowin M, Franus W (2017) Waste dolomite powder as an adsorbent of Cd, Pb(II), and Zn from aqueous solutions. Environ Earth Sci 76:521

GUS (2017) Environment. Statistical information and elaborations. Central Statistical Office, Warsaw https://stat.gov.pl/files/gfx/portalinformacyjny/pl/defaultaktualnosci/5484/1/18/1/ochrona_srodowiska_2017.pdf

Hashim MA, Mukhopadhyay S, Narayan Sahu J, Sengupta B (2011) Remediation technologies for heavy metal contaminated groundwater. J Environ Manag 92:2355–2388

Helios-Rybicka E, Wójcik R (2012) Competitive sorption/desorption of Zn, Cd, Pb, Ni, Cu, and Cr by clay-bearing mining wastes. Appl Clay Sci 65-66:6–13

Ho YS, McKay GA (1998) Comparison of chemisorption kinetic models applied to pollutant removal on various sorbents. Process Saf Environ Prot 76B:332–340

Hua M, Wang B, Chen L, Wang Y, Quynh VM, He B, Li X (2010) Verification of lime and water glass stabilized FGD gypsum as road sub-base. Fuel 89(8):1812–1817

Hua M, Zhang S, Pan B, Zhang W, Lv L, Zhang Q (2012) Heavy metal removal from water/wastewater by nanosized metal oxides: a review. J Hazard Mater 211:317–331

Huang J, Wu Z, Chen L, Sun Y (2015) The sorption of Cd(II) and U(VI) on sepiolite: a combined experimental and modeling studies. J Mol Liq 209:706–712

Hubicki Z, Kołodyńska D (2012) Selective removal of heavy metal ions from waters and waste waters using ion exchange methods. In: Kilislioğlu A (ed.), Ion exchange technologies. InTech. https://doi.org/10.5772/51040

Iskander AL, Khald EM, Sheta AS (2011) Zinc and manganese sorption behavior by natural zeolite and bentonite. Ann Agric Sci 56:43–48

ISO 15901:3–2007 Pore size distribution and porosity of solid materials by mercury porosimetry and gas adsorption—Part 3: Analysis of micropores by gas adsorption

Ivanets AI, Srivastava V, Kitikova NV, Shashkova IL, Silanpää M (2017) Non-apatite Ca-Mg phosphate sorbent for removal of toxic metal ions from aqueous solutions. J Environ Chem Eng 5:2010–2017

Jakimowicz-Hnatyszak K, Rubel S (1998) Wpływ przygotowania próbki na wyniki analityczne. Przegl Geol 46(9/2):903–909 (in Polish)

Kadirvelu K, Thamaraiselvi K, Namasivayam C (2001) Removal of heavy metals from industrial wastewaters by adsorption onto activated carbon prepared from an agricultural solid waste. Bioresour Technol 76(1):63–65

Kang J, Hu Y, Sun W, Liu R, Gao Z, Guan Q, Tang H, Yin Z (2018) Utilisation of FGD gypsum for silicate removal from scheelite flotation wastewater. Chem Eng J 341:272–279

Kotarska I (2012) Odpady wydobywcze z górnictwa miedzi w Polsce – bilans, stan zagospodarowania i aspekty środowiskowe. Cuprum 65:45–63 (in Polish)

Król M, Matras E, Mozgawa W (2016) Sorption of Cd2+ ions onto zeolite synthesized from perlite waste. Int J Environ Sci Tecnol 13(11):2697–2704

Kyzas GZ, Matis KA (2015) Nanoadsorbents for pollutants removal: a review. J Mol Liq 203:159–168

Langmuir I (1918) The adsorption of gases on plane surfaces of glass, mica and platinum. J Am Chem Soc 40:1361–1403

Lasheen MR, Ammar NS, Ibrahim HS (2012) Adsorption/desorption of Cd(II), Cu(II) and Pb(II) using chemically modified orange peel: equilibrium and kinetic studies. Solid State Sci 14:202–210

Li M, Zhang Z, Li R, Wang JJ, Ali A (2016) Removal of Pb(II) and Cd(II) ions from aqueous solution by thiosemicarbazide modified chitosan. Int J Biol Macromol 86:876–884

Liu P, Wang C-N, Song X-Y, Wu Y-N (2010) Dietary intake of lead and cadmium by children and adults – result calculated from dietary recall and available lead/cadmium level in food in comparison to result from food duplicate diet method. Int J Hyg Environ Health 213(6):450–457

Liu Y, Yana Y, Seshadri B, Qi F, Xuc Y, Bolanb N, Zheng F, Sun X, Han W, Wang L (2018) Immobilization of lead and copper in aqueous solution and soil using hydroxyapatite derived from flue gas desulphurization gypsum. J Geochem Explor 184:239–246

Łuczyńska J, Paszczyk B, Łuczyński MJ (2018) Fish as a bioindicator of heavy metals pollution in aquatic ecosystem of Pluszne Lake, Poland, and risk assessment for consumer's health. Ecotoxicol Environ Saf 153:60–67

Ma Z, Li Q, Yue Q, Gao B, Li W, Xu X, Zhong Q (2011) Adsorption removal of ammonium and phosphate from water by fertilizer controlled release agent prepared from wheat straw. Chem Eng J 171(3):1209–1217

Ma J, Qin G, Zhang Y, Sun J, Wang S, Jiang L (2018) Heavy metal removal from aqueous solutions by calcium silicate powder from waste coal fly-ash. J Clean Prod 182:776–782

Matusik J (2014) Arsenate, orthophosphate, sulfate and nitrate sorption equilibria and kinetics for halloysite and kaolinites with an induced positive charge. Chem Eng J 246:244–253

Maziarz P, Matusik J (2016) The effect of acid activation and calcination of halloysite on the efficiency and selectivity of Pb(II), Cd(II), Zn(II) and As(V) uptake. Clay Miner 51(3):385–394

Meitei MD, Prasad MNV (2014) Adsorption of Cu (II), Mn (II) and Zn (II) by Spirodela polyrhiza (L.) Schleiden: equilibrium, kinetic and thermodynamic studies. Ecol Eng 71:308–317

Meng Q, Chen H, Lin J, Lin Z, Sun J (2017) Zeolite A synthesized from alkaline assisted pre-activated halloysite for efficient heavy metal removal in polluted river water and industrial wastewater. J Environ Sci 56:254–262

Merrikhpour H, Jalali M (2012) Waste calcite sludge as an adsorbent for the removal of cadmium, copper, lead, and zinc from aqueous solutions. Clean Technol Environ Policy 14:845–855

Mikoda B, Gruszecka-Kosowska A (2018) Mineral and chemical characteristics, textural parameters, and the mobility of the selected elements of flotation waste, originating from the Polish copper-mining industry. Hum Ecol Risk Assess 24(5):1216–1232

Mikoda B, Gruszecka-Kosowska A, Klimek A (2017) Copper flotation waste from KGHM as potential sorbent for heavy metal removal from aqueous solutions. Hum Ecol Risk Assess 23(7):1610–1628

Milonjić SK (2007) A consideration of the correct calculation of thermodynamic parameters of adsorption. J Serb Chem Soc 72:1363–1367

Mohammadi M, Ghaemi A, Torab-Mostaedi M, Asadollahzadeh M, Hemmati A (2015) Adsorption of cadmium (II) and nickel (II) on dolomite powder. Desalin Water Treat 53:149–157

Namasivayam K, Kumuthu M (1998) Removal of direct red and acid brilliant blue by adsorption on to banana pith. Bioresour Technol 64:77–79

Patnukao P, Kongsuwan A, Pavasant P (2008) Batch studies of adsorption of copper and lead on activated carbon from Eucalyptus camaldulensis dehn. bark. J Environ Sci 20:1028–1034

Pehlivan E, Müjdat Özkan A, Dinc S, Parlayici S (2009) Adsorption of Cu2+ and Pb2+ ion on dolomite powder. J Hazard Mater 167:1044–1049

Qdais HA, Moussa H (2004) Removal of heavy metals from wastewater by membrane processes: a comparative study. Desalination 164(2):105–110

Rajasulochana P, Preethy V (2016) Comparison on efficiency of various techniques in treatment of waste and sewage water – a comprehensive review. Resource-Efficient Technologies 2(4):175–184

Rzepa G, Bajda T, Ratajczak T (2009) Utilization of bog iron ores as sorbents of heavy metals. J Hazard Mater 162:1007–1013

Sağ Y, Kutsal T (2000) Determination of the biosorption heats of heavy metal ions on Zoogloea ramigera and Rhizopus arrhizus. Biochem Eng J 6:145–151

Sari A, Tuzen M (2009) Kinetic and equilibrium studies of Pb(II) and Cd(II) removal from aqueous solution onto colemanite ore waste. Desalination 249:260–266

Senthil Kumar P, Ramalingam S, Sathyaselvabala V, Dinesh Kirupha S, Murugesan A, Sivanesan S (2012) Removal of cadmium(II) from aqueous solution by agricultural waste cashew nut shell. Korean J Chem Eng 29(6):756–768

Schwarz S, Schwarz D, Ohmann W, Neuber S (2018) Adsorption and desorption studies on reusing chitosan as an efficient adsorbent. Proceedings of the 3rd World Congress on Civil,

Structural, and Environmental Engineering (CSEE'18), Budapest, Hungary – April 8–10, 2018. https://doi.org/10.11159/awspt18.128

Shalaby NH, Ewais EMM, Elsaadany RM, Ahmed A (2017) Rice husk templated water treatment sludge as low cost dye and metal adsorbent. Egypt J Pet 26(3):661–668

Sherman J (1955) The theoretical derivation of fluorescent X-ray intensities from mixtures. Spectrochim Acta 7:283–306. https://doi.org/10.1016/0371-1951(55)80041-0

Shiraiwa T, Fujino N (1966) Theoretical calculation of fluorescent X-ray intensities in fluorescent X-ray spectrochemical analysis. Jpn J Appl Phys 5:886–899. https://doi.org/10.1143/JJAP.5.886

Sing KSW, Everett DH, Haul RAW, Moscou L, Pierotti RA, Rouquérol J, Siemieniewska T (1985) Reporting physisorption data for gas/solid systems with special reference to the determination of surface area and porosity. Pure Appl Chem 57:603–619

Srivastava P, Singh B, Angove M (2005) Competitive adsorption behavior of heavy metals on kaolinite. J Colloid Interface Sci 290:28–38

Taşar Ş, Kaya F, Özer A (2014) Biosorption of lead(II) ions from aqueous solution by peanut shells: equilibrium, thermodynamic and kinetic studies. J Environ Chem Eng 2: 1018–1026

Tchounwou PB, Yedjou CG, Patlolla AK, Sutton DJ (2012) Heavy metals toxicity and the environments. Heavy metal toxicity and the environment. In: Luch A (ed) Molecular, clinical and environmental toxicology. Experientia Supplementum, vol 101. Springer, Basel. https://doi.org/10.1007/978-3-7643-8340-4

Unuabonah EI, Olu-Owolabi BI, Fasuyi EI, Adebowale KO (2010) Modeling of fixed-bed column studies for the adsorption of cadmium onto novel polymer–clay composite adsorbent. J Hazard Mater 179(1–3):415–423

Yan Y, Dong X, Sun X, Sun X, Li J, Shen J, Han W, Liu X, Wang L (2014) Conversion of waste FGD gypsum into hydroxyapatite for removal of Pb2+ and Cd2+ from wastewater. J Colloid Interface Sci 429:68–76

Yan Y, Li Q, Sun X, Ren Z, He F, Wang Y, Wang L (2015) Recycling flue gas desulphurization (FGD) gypsum for removal of Pb(II) and Cd(II) from wastewater. J Colloid Interface Sci 457:86–95

Yang S, Ren X, Zhao G, Shi W, Montavon G, Grambow B, Wang X (2015) Competitive sorption and selective sequence of Cu(II) and Ni(II) on montmorillonite: batch, modeling, EPR and XAS studies. Geochim Cosmochim Acta 166:129–145

Yang Z, Tian S, Ji R, Liu L, Wang X, Zhang Z (2017) Effect of water-washing on the co-removal of chlorine and heavy metals in air pollution control residue from MSW incineration. Waste Manag 68:221–231